

A Report on Upgraded Seismic Monitoring Stations in Myanmar: Station Performance and Site Response

by Hrin Nei Thiam, Yin Myo Min Htwe, Tun Lin Kyaw, Pa Pa Tun, Zaw Min, Su Hninn Htwe, Tin Myo Aung, Kyaw Kyaw Lin, Myat Min Aung, Jason de Cristofaro, M. Franke, S. Radman, E. Lepiten, Emily Wolin, and Susan E. Hough

ABSTRACT

Myanmar is in a tectonically complex region between the eastern edge of the Himalayan collision zone and the northern end of the Sunda megathrust. Until recently, earthquake monitoring and research efforts have been hampered by a lack of modern instrumentation and communication infrastructure. In January 2016, a major upgrade of the Myanmar National Seismic Network (MNSN; network code MM) was undertaken to improve earthquake monitoring capability. We installed five permanent broadband and strong-motion seismic stations and real-time data telemetry using newly improved cellular networks. Data are telemetered to the MNSN hub in Nay Pyi Taw and archived at the Incorporated Research Institutions for Seismology Data Management Center. We analyzed station noise characteristics and site response using noise and events recorded over the first six months of station operation. Background noise characteristics vary across the array, but indicate that the new stations are performing well. MM stations recorded more than 20 earthquakes of $M \geq 4.5$ within Myanmar and its immediate surroundings, including an M 6.8 earthquake located northwest of Mandalay on 13 April 2016 and the M_w 6.8 Chauk event on 24 August 2016. We use this new dataset to calculate horizontal-to-vertical spectral ratios, which provide a preliminary characterization of site response of the upgraded MM stations.

Electronic Supplement: Figures of noise probability density functions of power spectral density, topographic profiles, and a schematic of the new vaults constructed by Regional Integrated Multi-Hazard Early Warning System (RIMES) at HKA and TMU.

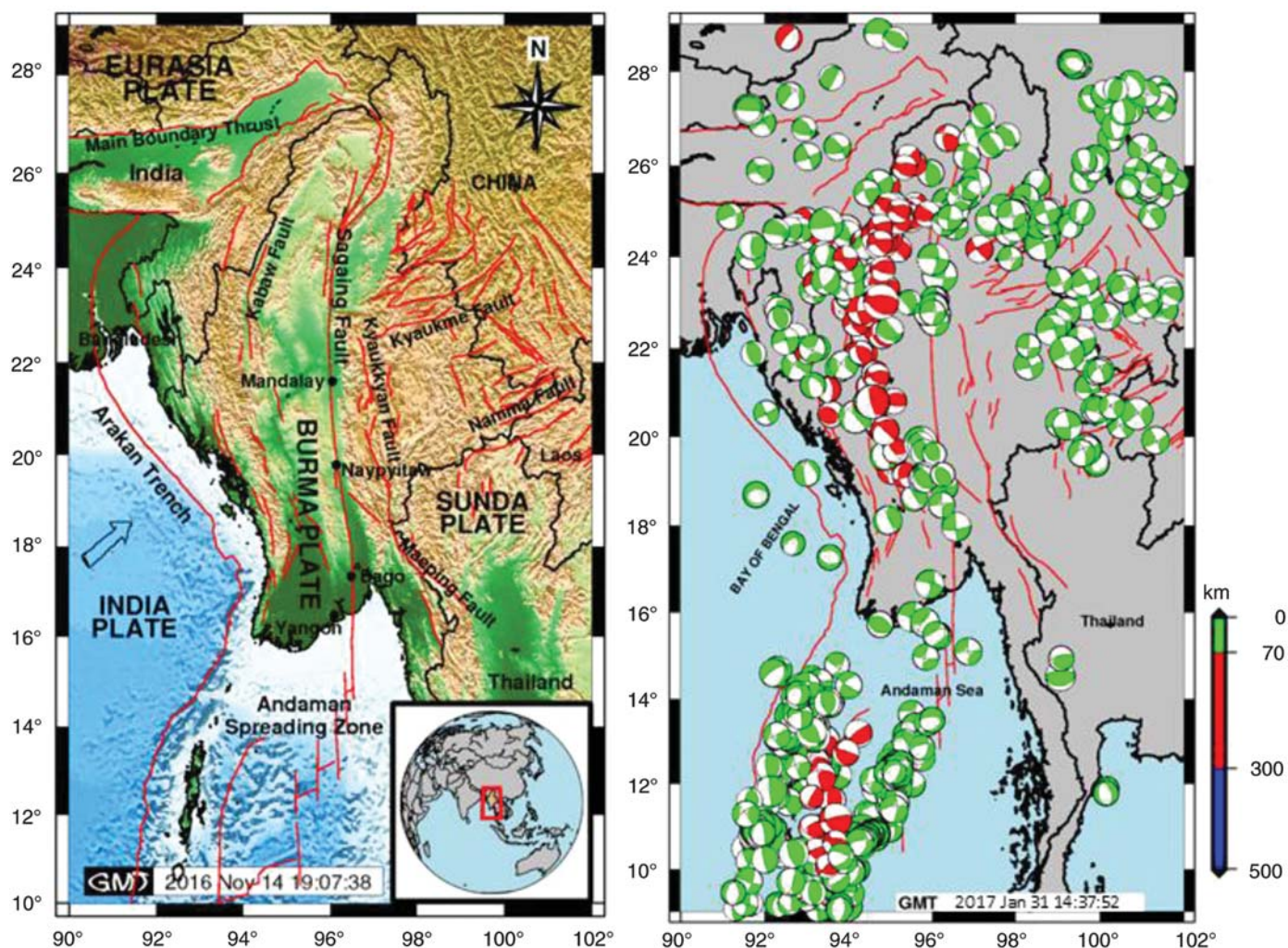
INTRODUCTION

Seismotectonics and Seismic Hazard

Myanmar lies along the Alpide belt, a zone of collision that extends from the northern Mediterranean eastward through Turkey, Iran, Afghanistan, and the Himalayas. This belt turns southward as it passes through Myanmar and finally terminates in Indonesia. Accordingly, Myanmar hosts a complex system of faults accommodating the collision between the Indian and Eurasian plates, with a convergence rate of ~ 49 mm/yr (DeMets *et al.*, 2010).

Broadly speaking, earthquakes in Myanmar are generated in two tectonic settings: (1) the continued subduction (with collision only in the north) of the northward-moving Indian plate underneath the Burma platelet, which is a part of the Eurasian plate (Steckler *et al.*, 2016); and (2) the northward movement of the Burma platelet from a spreading center in the Andaman sea (Thein and Swe, 2006). Global Positioning System measurements indicate that the relative motion between the Indian and Sunda plates is 35 mm/yr (Socquet *et al.*, 2006). Half of this motion is accommodated by the right-lateral strike-slip motion along the Sagaing fault, with the remainder taken up either by convergence at the Burma (or Arakan) subduction zone or localized deformation west of the Sagaing fault (Socquet *et al.*, 2006; Steckler *et al.*, 2016). Major sources of seismicity in Myanmar include the Kabaw fault zone along the Kabaw valley in western Myanmar, the well-known Sagaing fault, the Kyaukkyan fault situated east of Naungcho city, and a number of unnamed thrust faults in northwestern Myanmar (Thien *et al.*, 2009). In western Myanmar, earthquake focal depths delineate the subducting Indian plate, with seismicity reaching a maximum depth of about 150 km (Fig. 1; Thien *et al.*, 2009; Hurukawa *et al.*, 2012; Steckler *et al.*, 2016). Focal mechanisms (Fig. 1b) reflect the complex tectonic regime, with predominantly thrust mechanisms in the western part of the country and strike-slip motion along the Sagaing fault and in eastern Myanmar.

The right-lateral Sagaing fault stretches more than 1000 km through Myanmar, extending south from Putao to the west of Katha, through Sagaing, along the eastern flank



▲ **Figure 1.** (a) Seismotectonic map of Myanmar and surrounding regions, with major faults labeled; (b) centroid moment tensor (CMT) focal mechanisms, color-coded to indicate shallow, intermediate, and deep events between 1976 and 2016. Focal mechanisms were obtained from the Global CMT catalog (see [Data and Resources](#)).

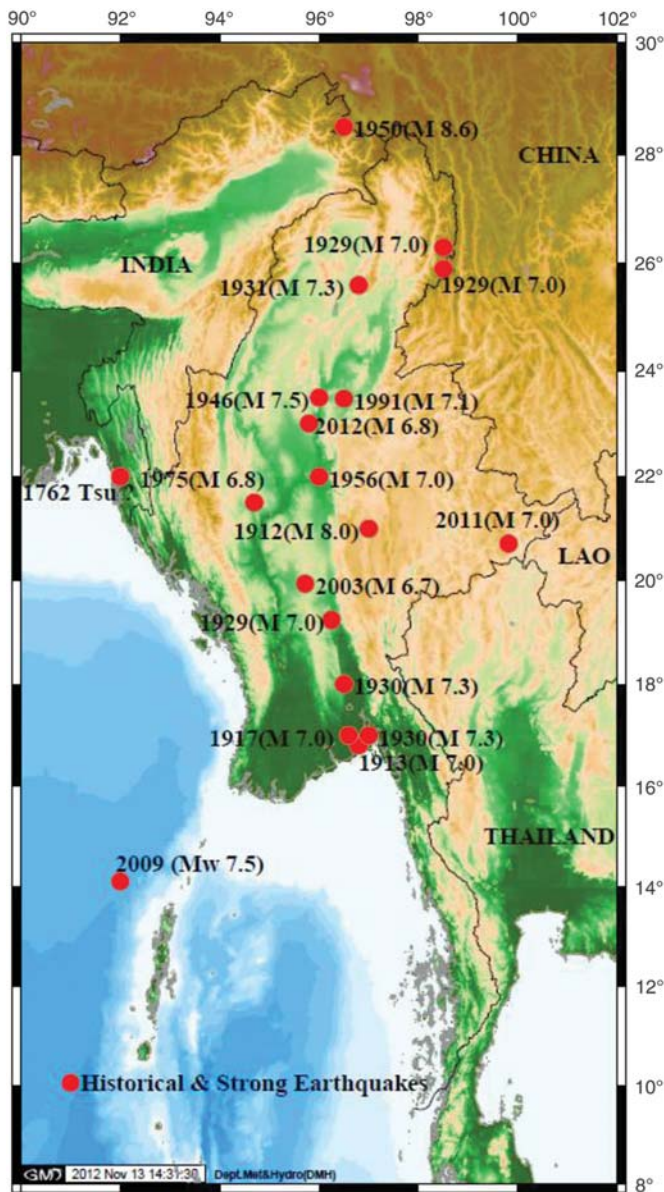
of Bago Yomas, then through Bago, and finally into the Gulf of Martaban (Thien *et al.*, 2009). A large portion of Myanmar's population of 51.5 million lives in close proximity to the Sagaing fault. Major population centers near the fault include the cities of Yangon (7.3 million residents), Mandalay (6.1 million residents), Bago (4.8 million residents), and the capital Nay Pyi Taw (1.1 million residents) (Department of Population, Ministry of Immigration and Population 2015).

Historical Seismicity

A number of destructive historical earthquakes occurred along the Sagaing fault in recent as well as historical times (Fig. 2; see also Aung, 2015, for a summary). The 5 May 1930 M_L 7.3 Bago earthquake caused the loss of about 500 lives at Bago, with major destruction and 50 lives at Yangon with some destruction. The 16 July 1956 M_L 7.0 Sagaing earthquake caused damage to religious edifices and buildings at Sagaing. The 8 July 1975 M_L 6.8 Bagan earthquake caused destruction to many historical pagodas at Bagan and two fatalities. The dam-

age to the temples at Bagan was considered a major loss of religious heritage by the people of Myanmar; damage remains evident to this day. More recently, the 5 January 1991 M_L 7.1 Tagaung earthquake caused moderate destruction to the surrounding area. Myanmar's largest earthquake in recent history occurred on the Kyaukkyan fault in 1912, with an estimated magnitude of 8.0. This event caused severe damage in the city of Maymyo (presently known as Pyin Oo Lwin). Railroad tracks were bent where they crossed the fault, and massive landslides occurred. Aftershocks continued for six months.

More recently, a number of moderately large earthquakes occurred in Myanmar, including an M_w 6.9 earthquake on 24 March 2011 in eastern Myanmar near the Thai border and the M_w 6.8 Shwebo earthquake on 11 November 2012. Both of these events caused significant local damage and claimed dozens of lives. Two events of similar size occurred in 2016: an M_w 6.9 event in western Myanmar on 13 April and an M_w 6.8 event near Chauk on 24 August 2016. Both of these events were relatively deep, with estimated depths of 135 and 84 km, respectively, which mitigated



▲ **Figure 2.** Historical and recent significant events in Myanmar prior to the completion of the network upgrade project.

their impact. The Chauk earthquake, however, damaged temples in the nearby city of Bagan, and caused four fatalities.

Although recent as well as historic earthquakes demonstrate that seismic hazard is clearly high in Myanmar, understanding of the seismotectonic framework and characterization of seismic hazard have been hampered by limited availability of modern digital seismic data. In this report, we describe a major upgrade of the national seismic network that was completed in 2016, including initial characterization of noise levels and site response at five upgraded monitoring sites.

PAST SEISMIC MONITORING

The Department of Meteorology and Hydrology (DMH) has conducted seismological monitoring activities since 1963. For

much of that time, real-time monitoring was difficult due to the use of analog instruments and a lack of suitable or affordable infrastructure for data telemetry. Three-component Katsujima analog seismographs were installed in Yangon in 1976 and in Mandalay in 1977. Solar-powered velocity-type seismographs were installed at Sittwe in 1984 and in Dawei in 1985. Three of these analog seismograph stations (Yangon, Mandalay, and Dawei) are still functioning. Very-small-aperture terminal (VSAT) telemetry was installed at Sittwe in 2011; however, telemetry has not been operational since 2015. Eleven Etna strong-motion accelerographs were installed throughout Myanmar, including 10 installed in 2001 and one installed in Nay Pyi Taw in 2009. As of January 2016, five of these instruments were operational, but none are telemetered.

Four sets of digital seismographs were installed in DMH facilities at Yangon and Mandalay in April 2002 and at Myitkyina and Namsan in 2008. These instruments were donated by the Yunnan Earthquake Administration (formerly the Yunnan Seismic Bureau) and China Earthquake Administration, People's Republic of China. The stations in Mandalay and Yangon stopped working in 2004 due to lightning strikes. Data from the Myitkyina and Namsan stations are not currently available due to problems with the satellite communication system. The Thailand-based Regional Integrated Multi-Hazard Early Warning System (RIMES) installed one broadband station at Sittwe (RM.SIM) in 2009; these data are available through the Incorporated Research Institutions for Seismology Data Management Center (IRIS-DMC). In 2009, the DMH installed three Guralp CMG-3ESPC broadband seismometers at Nay Pyi Taw, Patheingyi, and Hpa-an. At present, data from these instruments are archived at the DMH but not used in real-time monitoring.

In addition to seismic instrumentation, two sea-level tide gauges are installed at Mawlamyine and Sittwe for tsunami warning. These instruments were donated in 2006 by the International Oceanographic Commission of the United Nations Educational, Scientific, and Cultural Organization (IOC-UNESCO). An additional sea-level station was installed at Hingyi-kun during the Japan International Cooperation Agency end-to-end early warning system project in October 2014.

Before the network upgrade of 2016, real-time monitoring of earthquakes in Myanmar relied almost exclusively on data from other networks, including the Thai Seismic Monitoring Network, the National Seismic Network of India, and the Global Seismic Network (see [Data and Resources](#)). Beginning in 2013, SeisComp3 ([Hanka et al., 2010](#)) has been used for data acquisition and automatic event location.

NETWORK UPGRADE

In January 2016, we completed a major network upgrade to improve the DMH's capacity to monitor earthquakes within Myanmar. This upgrade was the culmination of a 3-yr effort to identify suitable sites, complete vault construction, and explore potential options for data telemetry. These new stations have been registered with the International Federation of Digital



▲ **Figure 3.** Installations of Keng Tung (KTN) and Tamu (TMU). (a) Existing small concrete building in Keng Tung (KTN) with (b) newly constructed instrument pier. (c) Newly constructed vault in Tamu (TMU) and (d) Tamu (TMU) vault interior.

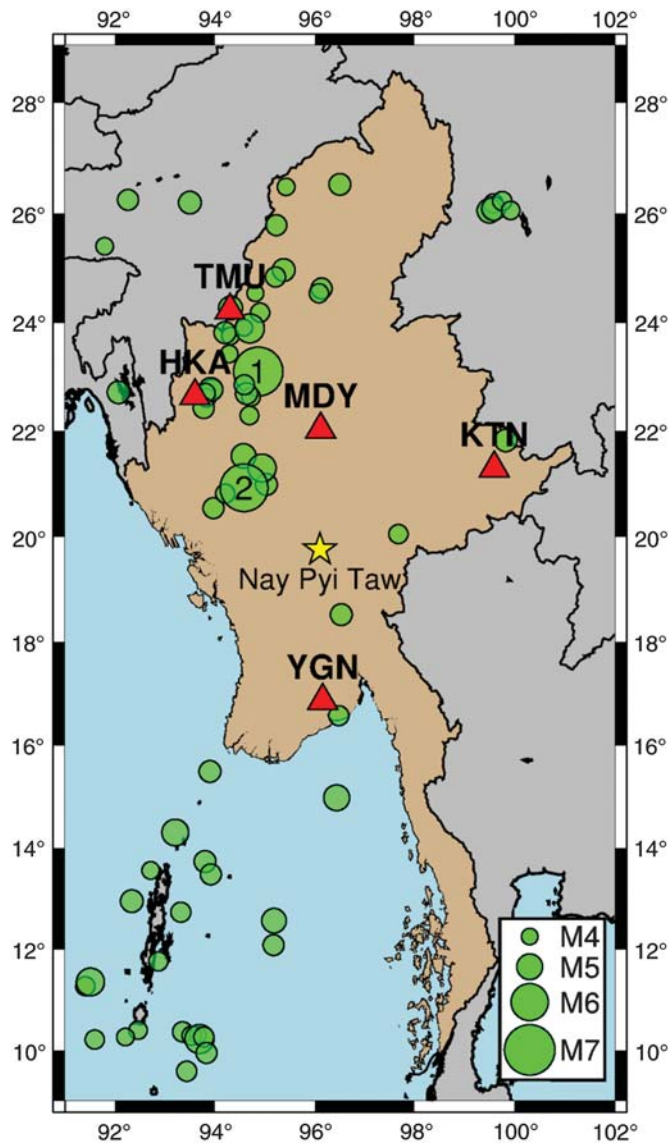
Seismograph Networks (FDSN) with network code MM and DOI (see [Data and Resources](#)).

Existing stations in Mandalay (MM.MDY) and Yangon (MM.YGN), installed in World-Wide Standard Seismographic Network (WWSSN)-era seismic vaults, were upgraded. At Keng Tung (MM.KTN), an instrument pier was constructed within an existing small concrete building that had been built earlier to house instrumentation (Fig. 3a,b). New shallow outdoor vaults were constructed at Tamu (MM.TMU) and Hakha (MM.HKA) (Fig. 3c,d and © Fig. S4, available in the electronic supplement to this article). To facilitate permitting and site maintenance, all of the sites are located at DMH offices at locations that provide a good distribution for regional seismic monitoring (Fig. 4). These locations include a variety of site conditions. MDY is located on Mandalay Hill, an isolated hard-rock site within the Ayeyawaddy valley that has long been a site of religious and cultural significance. KTN and HKA are located in mountainous regions in eastern and western Myanmar, respectively.

Both are expected to be hard-rock or thin-sediment sites. YGN and TMU are sediment sites within the Ayeyawaddy delta and Kabaw valley, respectively.

Each station is instrumented with a Streckeisen STS-2.5 broadband sensor, a Kinematics ES-T Episensor strong-motion accelerometer, and a Quanterra Q330 datalogger with an environmental processor including a Setra 278 barometer. Data from both the broadband and strong-motion instruments are recorded at 1 and 100 samples per second. The sensors are installed on a 2.5-m-deep concrete pier, with piles driven into the ground below to a depth of 1 m or to bedrock. Data from all five upgraded stations are telemetered via a cellular modem to the network hub at the DMH office in Nay Pyi Taw, where they are received, processed, and archived by Kinematics' real-time Aspen software system. Beginning in May 2016, data are also telemetered to the IRIS-DMC, where they are freely available in real time.

With the upgraded instrumentation and software, real-time data from MM stations and other local and regional networks



▲ **Figure 4.** Map showing locations of newly upgraded stations in the MM network (red triangles, see the [Network Upgrade](#) section for details), the network hub in Nay Pyi Taw (yellow star), and earthquakes with $M \geq 4$ that occurred after the network upgrade in January 2016 (green circles) (epicenters from U.S. Geological Survey Advanced National Seismic System Comprehensive Catalog; see [Data and Resources](#)). Numbered events indicate epicenters of M_w 6.8 events: (1) 13 April 2016 and (2) 24 August 2016.

are received by the real-time Aspen system and forwarded to two SeisComP3 systems ([Weber et al., 2007](#)) previously installed at the DMH. Seismic events are detected and located automatically by Antelope (integrated into Aspen) and SeisComp3, then reviewed by an analyst to refine phase picks and event locations. Earthquake bulletins are usually issued within 10–20 min of a detection. The SeisComP3 systems routinely detect earthquakes of M 4.0 and above within Myanmar. The detection threshold of the Aspen system is slightly lower at M 3.9, with some events as small as 3.5 detected within Myanmar (mostly in the north

and northwest). The Aspen system requires a minimum of four stations for a detection. Analysts at the DMH also manually review data using SeisAn ([Havskov and Ottemoller, 1999](#)) and are able to detect events as small as magnitude 2.5 using one or two stations.

The DMH also monitors the seismicity of the Indian Ocean region for potentially tsunamigenic earthquakes. The new and upgraded instruments enhance this critical real-time monitoring capability.

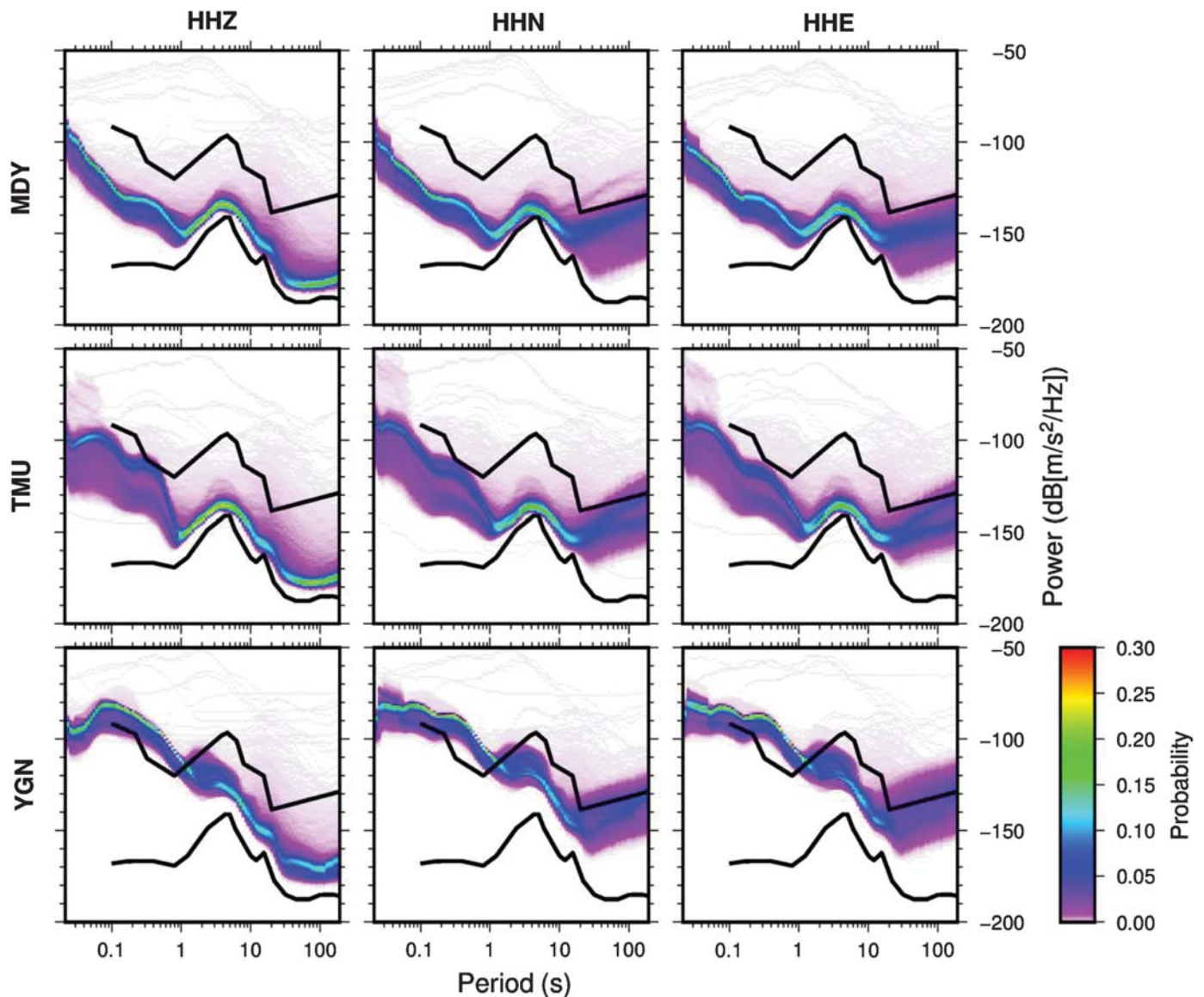
The 13 April 2016 and 24 August 2016 events occurred following the completion of the network upgrade described in this report. Both were successfully recorded by all five upgraded monitoring sites. Analysis of these events is ongoing, to be presented in subsequent reports.

STATION PERFORMANCE

We assess the noise characteristics of the broadband sensors at the five upgraded stations by examining probability density functions (PDFs) of power spectral density (PSD). These plots, calculated using the method of [McNamara and Buland \(2004\)](#), are available from the IRIS-DMC. We used the DMC’s noise-PDF webservice to request PDF PSD plots including all data available at the DMC (May 2016–December 2016). These are shown in [Figure 5](#) and [Figure S1](#).

Noise varies greatly from station to station. At periods > 20 s, the mode of power for the vertical component of all stations falls within 10–20 dB of the new low noise model (NLNM; [Peterson, 1993](#)). Horizontal long-period noise is lowest at TMU and MDY, whereas noise at YGN and HKA often exceeds the new high noise model (NHNM; [Peterson, 1993](#)). TMU and KTN display bimodal behavior, suggesting diurnal variations in long-period noise levels.

Cultural noise (periods 0.1–1 s) varies drastically between stations. MDY has the lowest cultural noise. YGN has a high level of high-frequency energy, with noise levels often exceeding the NHNM by 10–20 dB. Cultural noise at HKA, TMU, and KTN approaches and sometimes exceeds the NHNM levels. At these three stations, there is a 20–30 dB variation in noise levels, which may be due to differences in human activity in the day and night. At YGN, noise levels consistently exceed the NHNM, likely due to a combination of cultural noise produced by the 4 million residents of Yangon and the city’s location on delta sediments. Long-period noise can also potentially be generated by minute tilting of the seismic pier, which can result from unconformity of material beneath the pier (e.g., [Uhrhammer et al., 1998](#)). This effect might be an issue for the stations with newly constructed vaults or piers (TMU, HKA, and KTN); it is less likely to affect long-period noise levels at the stations (YGN, MDY) installed in WWSSN-era vaults. Further investigations of noise levels, including exploration of the diurnal and seasonal variability of noise at all stations, will be undertaken once more data are collected.

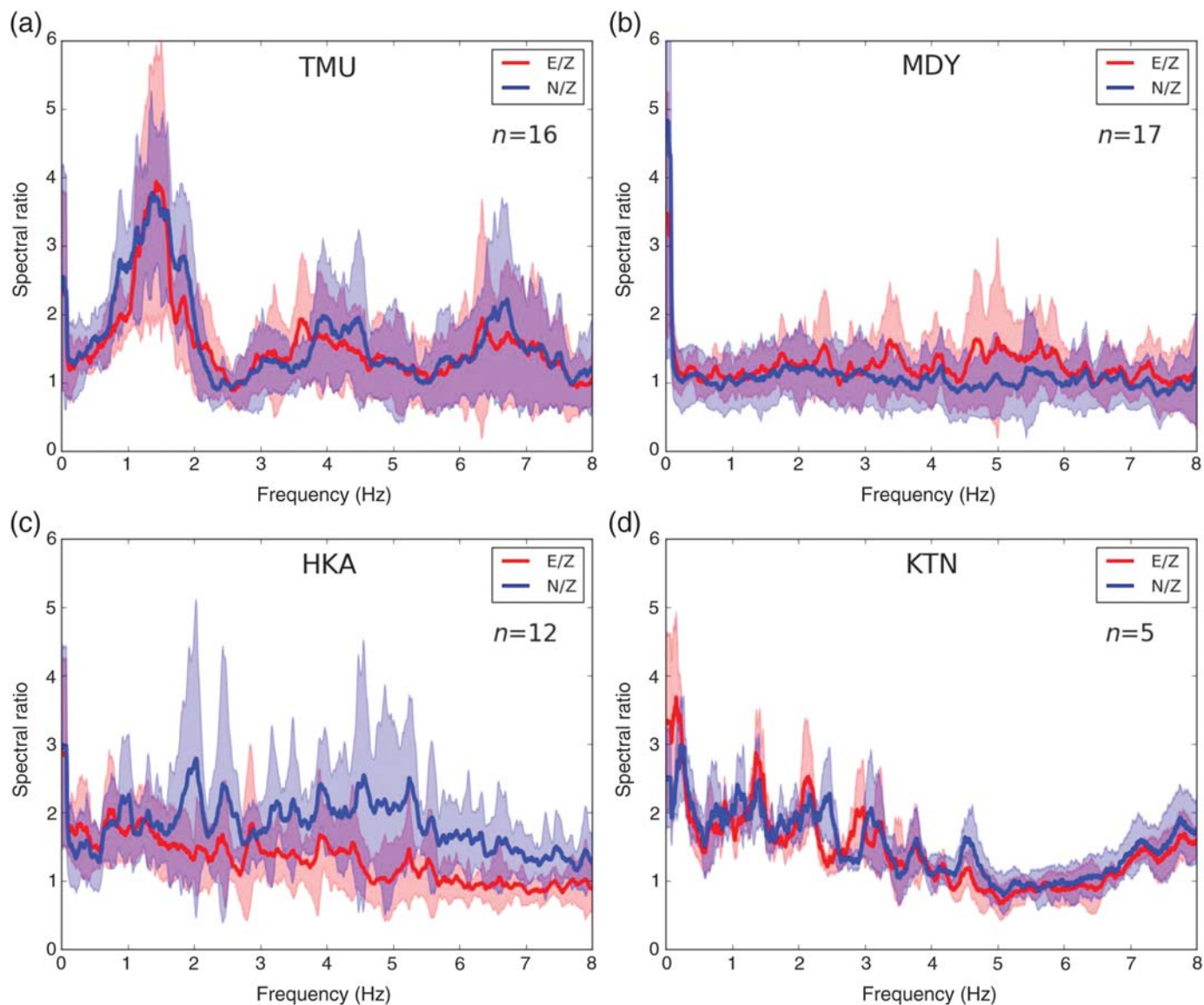


▲ **Figure 5.** Noise probability density functions of power spectral density plots for May 2016 to December 2016 for upgraded stations. Separate panels show results for each station; from top to bottom, MDY, TMU, and YGN. For each station, results for each separate component are shown; from left to right: vertical, north–south, and east–west. Solid black lines indicate new high noise model and new low noise model from [Peterson \(1993\)](#).

SITE RESPONSE

Ambient noise levels at each station reflect the level of cultural noise but also potentially the local site response due to sediment-induced amplification ([Field *et al.*, 1990](#)). At the present time, apart from the general geological assessments mentioned earlier, site characterizations are unavailable for the upgraded network sites, but two (YGN and TMU) are soft-sediment sites where significant amplification is expected (see © Figs. S2 and S3 for topographic profiles at each station). Although ambient noise can be used to investigate site response, the seismicity rate in Myanmar is high enough that we analyze data from earthquakes recorded by the upgraded stations: between January 2016 and July 2016, the upgraded stations have recorded

more than 20 earthquakes with $M \geq 4.5$ within Myanmar and the immediate area. Although a full characterization of site response will be undertaken once a larger dataset has been recorded, for this report we analyze data from these events to determine horizontal-to-vertical (H/V) spectral ratios (HVSr; [Lermo and Chavez-Garcia, 1993](#)) at each of the five stations. Following seminal studies by [Nakamura \(1989\)](#) (using ambient noise) and [Lermo and Chavez-Garcia \(1993\)](#) (using earthquake recordings), the HVSr method has been used extensively to investigate sediment-induced amplification, using both ambient noise and earthquake recordings. [Chavez-Garcia *et al.* \(1996\)](#) further showed that H/V ratios can also potentially reveal resonances associated with topographic amplification. For each event, we selected a 15-min window of data



▲ **Figure 6.** Average horizontal-to-vertical spectral ratio results for earthquakes well recorded at (a) TMU, (b) MDY, (c) HKA, and (d) KTN. Average ratios are calculated separately using E–W/Z (red) and N–S/Z (blue); number of events used at each station is indicated. Solid lines indicate mean; shaded region shows ± 1 standard deviation.

around the event, using data sampled at 100 samples per second. We visually inspected the traces and discarded records with a low signal-to-noise ratio (SNR). TMU recorded 16 events; MDY recorded 17; HKA recorded 12; and KTN recorded 5. Only two events were recorded at YGN due to the high level of cultural noise.

Using the Seismic Analysis Code (SAC) (Goldstein and Snoke, 2005), we removed the mean from each trace, applied a 5% cosine taper to both ends, and took the Fourier transform. We applied smoothing to the resulting spectra using a moving average of the neighboring 100 points. To calculate HVSRs, we divided the spectra from the north–south (N–S) and east–west (E–W) components by the spectrum from the vertical (Z) component. N–S/Z spectra and E–W/Z spectra are shown in Figure 6 for MDY, TMU, HKA, and KTN. Results are

not shown for YGN because too few earthquakes have been recorded at this station with sufficient SNRs for analysis.

TMU displays a strong peak around 1.5 Hz and smaller peaks around 4 and 6.5 Hz, consistent with expectations for site amplification associated with shallow fluvial sediments. At MDY, H/V ratios are close to 1, indicating very little amplification. This is consistent with the station’s location at the base of Mandalay Hill, an expected hard-rock site. Although ratios are not as consistently low at HKA, this station also reveals no significant site response. At Hakha, the E–W/Z and N–S/Z ratios are somewhat different, with the E–W/Z curve close to 1.5 and the N–S/Z closer to a ratio of 2. It is possible that the observed amplification is associated with topographic effects at this site; HKA’s location on a saddle in a mountainous area may further account for differences between N–S and

E–W ground motions. KTN has a peak around 1.2 Hz and perhaps a smaller shoulder at 2 Hz. This may indicate that thin sediments are present at the site; the station is located on the edge of a basin, but thickness of sediment at the site is not presently known. Further work will be needed to fully characterize the site conditions at each of the stations and to investigate site response.

CONCLUSIONS

Although it has long been recognized that Myanmar lies along an active plate boundary zone, understanding of the complex seismotectonic framework and characterization of seismic hazard have been hampered by a lack of modern instrumental seismic data. To supplement efforts taken in recent years to improve seismic monitoring, we undertook a significant upgrade of the network, including installation of state-of-the-art sensors and other instrumentation at five stations with real-time telemetry to an upgraded network hub in Nay Pyi Taw. Because of the high rate of seismicity in Myanmar, a rapidly growing volume of broadband and strong-motion data are now being collected. In this report, we present a preliminary analysis of noise analysis and HVSR to assess station performance and illuminate the nature of local site response at each of the monitoring stations. Data from the upgraded network will provide an invaluable resource to improve our understanding of the complex seismotectonic framework and seismic hazard in Myanmar. Detailed analysis of recently recorded large earthquakes, including the 13 April 2016 and 24 August 2016 events, is ongoing and will be reported in subsequent reports.

DATA AND RESOURCES

Data from the upgraded stations of the Myanmar National Seismic Network are available from the Incorporated Research Institutions for Seismology Data Management Center (IRIS-DMC) with network code MM (Department of Meteorology and Hydrology—National Earthquake Data Center, 2016). Other stations used by the Department of Meteorology and Hydrology (DMH) for seismic monitoring in Myanmar are operated by Regional Integrated Multi-Hazard Early Warning System (RIMES; RM; Regional Integrated Multi-Hazard Early Warning System [RIMES Thailand], 2008), the Thai Seismic Monitoring Network (TM; <http://www.fdsn.org/networks/detail/TM>, last accessed February 2017), the Malaysian National Seismic Network (MY; <http://www.fdsn.org/networks/detail/MY>, last accessed February 2017), the National Seismic Network of India (IN; <http://www.fdsn.org/networks/detail/IN/>, last accessed February 2017), the Global Seismic Network, including IRIS/IDA (II; Scripps Institution of Oceanography, 1986) and IRIS/U.S. Geological Survey (USGS) (IU; Albuquerque Seismological Laboratory (ASL)/USGS, 1988), and the New China Digital Seismograph Network (IC; Albuquerque Seismological Laboratory (ASL)/USGS, 1992; <http://www.fdsn.org/networks/detail/IC>, last accessed February 2017). Data analysis and figure production were done with Seismic Analysis Code

(Goldstein and Snoke, 2005), Generic Mapping Tools (GMT; Wessel *et al.*, 2013), ObsPy (Beyreuther *et al.*, 2010), and Matplotlib (Hunter, 2007). Focal mechanisms in Figure 1 were obtained by searching the Global Centroid Moment Tensor Project database (www.globalcmt.org, last accessed August 2016) (Dziewonski *et al.*, 1981; Ekström *et al.*, 2012). Earthquake epicenters in Figure 4 are from the USGS Advanced National Seismic System (ANSS) Comprehensive Catalog (<http://earthquake.usgs.gov/earthquakes/search>, last accessed August 2016). ☒

ACKNOWLEDGMENTS

We thank Daniel McNamara, Valerie Thomas, an anonymous reviewer, and the Associate Editor for constructive reviews that improved this article. The network upgrade is supported by the U.S. Agency for International Development, Office of Foreign Disaster Assistance, and the Myanmar Ministry of Transport. We thank United States Agency for International Development (USAID), the U.S. Department of State, and the Government of Myanmar for the logistical and financial support that made this project possible.

Any use of trade, firm, or product names is for descriptive purposes only and does not imply endorsement by the U.S. Government.

REFERENCES

- Albuquerque Seismological Laboratory (ASL)/USGS (1988). Global Seismograph Network (GSN—IRIS/USGS), *International Federation of Digital Seismograph Networks*, Other/Seismic Network, doi: 10.7914/SN/IU.
- Albuquerque Seismological Laboratory (ASL)/USGS (1992). New China Digital Seismograph Network, *International Federation of Digital Seismograph Networks*, Other/Seismic Network, doi: 10.7914/SN/IC.
- Aung, H. H. (2015). *Myanmar Earthquake History*, Myanmar Engineering Society, Yangon, Myanmar, 91 pp., https://www.researchgate.net/publication/275466080_Myanmar_Earthquakes_History (last accessed February 2017).
- Beyreuther, M., R. Barsch, L. Krischer, T. Megies, Y. Behr, and J. Wassermann (2010). ObsPy: A Python toolbox for seismology, *Seismol. Res. Lett.* **81**, no. 3, 530–533.
- Chavez-Garcia, F. J., L. R. Sanchez, and D. Hatzfeld (1996). Topographic site effects and HVSR. A comparison between observations and theory, *Bull. Seismol. Soc. Am.* **86**, no. 5, 1559–1573.
- DeMets, C., R. G. Gordon, and D. F. Argus (2010). Geologically current plate motions, *Geophys. J. Int.* **181**, no. 1, 1–80.
- Department of Population, Ministry of Immigration and Population (2015). The 2014 Myanmar Population and Housing Census, *The Union Report, Census Report*, Vol. 2.
- Department of Meteorology and Hydrology—National Earthquake Data Center (2016). Myanmar National Seismic Network, *International Federation of Digital Seismograph Networks*, Other/Seismic Network, doi: 10.7914/SN/MM.
- Dziewonski, A. M., T.-A. Chou, and J. H. Woodhouse (1981). Determination of earthquake source parameters from waveform data for studies of global and regional seismicity, *J. Geophys. Res.* **86**, no. B4, 2825–2852, doi: 10.1029/JB086iB04p02825.
- Ekström, G., M. Nettles, and A. Dziewonski (2012). The global CMT project 2004–2010: Centroid-moment tensors for 13,017 earthquakes, *Phys. Earth Planet. In.* **200/201**, 1–9, doi: 10.1016/j.pepi.2012.04.002.

- Field, E. H., S. E. Hough, and K. H. Jacob (1990). Using micro-tremors to assess potential earthquake site response: A case study in Flushing Meadows, New York, *Bull. Seismol. Soc. Am.* **80**, no. 6, 1456–1480.
- Goldstein, P., and A. Snoko (2005). SAC availability for the IRIS community, *Incorporated Institutions for Seismology Data Management Center Electronic Newsletter* **7**, no. 1.
- Hanka, W., J. Saul, B. Weber, J. Becker, P. Harjadi, Fauzi, and GITEWS Seismology Group (2010). Real-time earthquake monitoring for tsunami warning in the Indian Ocean and beyond, *Nat. Hazards Earth Syst. Sci.* **10**, 2611–2622, doi: [10.5194/nhess-10-2611-2010](https://doi.org/10.5194/nhess-10-2611-2010).
- Havskov, J., and L. Ottemøller (1999). SeisAn earthquake analysis software, *Seismol. Res. Lett.* **70**, no. 5, 523–534, doi: [10.1785/gssrl.70.5.532](https://doi.org/10.1785/gssrl.70.5.532).
- Hunter, J. D. (2007). Matplotlib: A 2D graphics environment, *Comput. Sci. Eng.* **9**, no. 3, 90–95.
- Hurukawa, N., P. P. Tun, and B. Shibazaki (2012). Detailed geometry of the subducting Indian Plate beneath the Burma Plate and subcrustal seismicity in the Burma Plate derived from joint hypocenter relocation, *Earth Planets Space* **64**, 333–343, doi: [10.5047/eps.2011.10.011](https://doi.org/10.5047/eps.2011.10.011).
- Lermo, J., and F. J. Chavez-Garcia (1993). Site effect evaluation using spectral ratios with only one station, *Bull. Seismol. Soc. Am.* **83**, no. 5, 1574–1594.
- McNamara, D. E., and R. P. Buland (2004). Ambient noise levels in the continental United States, *Bull. Seismol. Soc. Am.* **94**, no. 4, 1517–1527.
- Nakamura, Y. (1989). A method for dynamic characteristics estimation of subsurface using microtremor on the ground surface, *Railw. Tech. Res. Inst. Q. Rept.* **30**, no. 1, 25–33.
- Peterson, J. (1993). Observations and modeling of seismic background noise, *U.S. Geol. Surv. Open-File Rept.* 93-322, U.S. Department of the Interior, U.S. Geological Survey.
- Regional Integrated Multi-Hazard Early Warning System (RIMES Thailand) (2008). Regional Integrated Multi-Hazard Early Warning System, *International Federation of Digital Seismograph Networks, Other/Seismic Network*, doi: [10.7914/SN/RM](https://doi.org/10.7914/SN/RM).
- SeisAn (2005). IRIS/IDA Seismic Network, *International Federation of Digital Seismograph Networks, Other/Seismic Network*, doi: [10.7914/SN/II](https://doi.org/10.7914/SN/II).
- Socquet, A., C. Vigny, N. Chamot-Rooke, W. Simons, C. Rangin, and B. Ambrosius (2006). India and Sunda plates motion and deformation along their boundary in Myanmar determined by GPS, *J. Geophys. Res.* **111**, no. B5, doi: [10.1029/2005JB003877](https://doi.org/10.1029/2005JB003877).
- Steckler, M. S., D. R. Mondal, S. H. Akhter, L. Seeber, L. Feng, J. Gale, E. M. Hill, and M. Howe (2016). Locked and loading megathrust linked to active subduction beneath the Indo-Burman Ranges, *Nature Geosci.* **9**, 615–618, doi: [10.1038/ngeo2760](https://doi.org/10.1038/ngeo2760).
- Thein, M., and T. L. Swe (2006). *Seismic Zone Map of Myanmar (Rev. Vers., 2005)*, prepared under the auspices of Myanmar Earthquake Committee.
- Thien, M., T. Myint, S. T. Tun, and T. L. Swe (2009). Earthquake and tsunami hazard in Myanmar, *J. Earthq. Tsunami* **3**, no. 2, doi: [10.1142/S1793431109000482](https://doi.org/10.1142/S1793431109000482).
- Uhrhammer, R. A., W. Karavas, and B. Romanowicz (1998). Broadband seismic station installation guidelines, *Seismol. Res. Lett.* **69**, no. 1, 16–26.
- Weber, B., J. Becker, W. Hanka, A. Heinloo, M. Hoffmann, T. Kraft, D. Pahlke, J. Reinhardt, J. Saul, and H. Thoms (2007). SeisComp3—Automatic and interactive real time data processing, *Geophys. Res. Abstr.* **9**, 09219.
- Wessel, P., W. H. F. Smith, R. Scharroo, J. Luis, and F. Wobbe (2013). Generic Mapping Tools: Improved version released, *EOS Trans. AGU* **94**, no. 45, 409–410.

*Hrin Nei Thiam
Yin Myo Min Htwe
Tun Lin Kyaw
Pa Pa Tun
Zaw Min
Su Hninn Htwe
Tin Myo Aung
Kyaw Kyaw Lin
Myat Min Aung
Department of Meteorology and Hydrology
Lewe Lane Haung Road
Pyinmana, Nay Pyi Taw
Myanmar*

*Jason de Cristofaro
Emily Wolin
Susan E. Hough
U.S. Geological Survey
525 South Wilson Avenue
Pasadena, California 91106 U.S.A.
hough@usgs.gov*

*M. Franke
S. Radman
Kinematics
222 Vista Avenue
Pasadena, California 91107 U.S.A.*

*E. Lepiten
RIMES
Khlung Nung, Khlung Luang District
Pathum Thani 1201
Bangkok, Thailand*

Published Online 22 March 2017